Multi-UAV Placement Strategy for Disaster-Resilient Communication Network

Mansi Peer, Vivek Ashok Bohara, Anand Srivastava
Wirocomm Research Group,
Department of Electronics and Communication Engineering
Indraprastha Institute of Information Technology, Delhi (IIIT-Delhi), India 110020
Email: mansip@iiitd.ac.in, vivek.b@iiitd.ac.in, anand@iiitd.ac.in

***Abstract*—Unmanned aerial vehicles (UAVs) have the potential of being used as flying base stations to facilitate a disaster-resilient communication network. However, the optimal placement of UAVs over a disaster-affected area must be aware of the mobility of the ground users. Hence, in this paper, we propose a ground user mobility aware multi-UAV placement strategy for disaster-resilient communication network. We formulate an optimization problem to maximize the number of ground users covered by the UAVs, while also taking into account the UAV flight time constraint. Specifically, in this work, the emergency first responders (EFRs) are considered as the ground users and their mobility is modeled in the disaster-affected area. We analyze single-UAV and multi-UAV scenarios in terms of average covered users and average coverage time. We observe that there exists a trade-off between the average number of covered users and average coverage time.**

***Index Terms*—Unmanned Aerial Vehicles (UAV), Disaster-Resilient Communication, Ground User Mobility Modeling, UAV Placement Optimization**

I. Introduction

In the aftermath of disasters, man-made or natural, it is imperative to carry out search and rescue to save as many lives as possible. The search and rescue team members that arrive at the disaster location need to maintain effective communication among themselves as well as with the far-off disaster control room for sharing the updates. However, the existing wireline and mobile communication services generally become non-operational in disaster area. For instance, approximately 1.9 million fixed communication lines and 29,000 base stations were damaged during the Japan tsunami in 2011 [1]. At present, the search and rescue teams depend on the legacy public safety communication networks like terrestrial trunked radio (TETRA) in Europe and association of public-safety communications officials (APCO 25) in US that support only voice services [2]. It has been suggested that the public safety communication networks need to be upgraded with emerging technologies that can support both voice and multimedia broadband services. The third generation partnership project (3GPP) Releases 13-15 recommend the adoption of long term evolution (LTE) technology for the public safety communication [3]. Further, recent studies have also demonstrated that the communication coverage in the disaster scenarios can be enhanced by employing unmanned aerial vehicles (UAVs) which helps in establishing disaster-resilient communication networks due to their flexibility and maneuverability [4]. Moreover, UAVs are capable of offering low-latency communication services.

With the recent technological advances, it is feasible to deploy UAVs for the roles of flying/aerial base stations (BSs) as well as aerial user equipments (UEs) [4]. Specifically, on using UAVs as flying BSs, the key challenge is the optimal three-dimensional (3-D) placement of the UAVs for efficient network performance [5]. The 3-D placement of UAVs has drawn a lot of attention from the researchers over the last few years. For instance, authors in [6] have dealt with maximization of covered users via optimal 3-D placement of a single UAV. In [7], the optimal 3-D deployment of multiple UAVs is investigated to maximize the downlink coverage performance with minimum transmit power. In [8] and [9], 3-D placement UAV-BSs is studied for maximizing the sum logarithmic rate of the users and effectively prolonging the life-time of the network, respectively. Further, they analyzed the network performance for different user distributions such as Poisson point process and clustered user distribution.

However, the current literature on 3-D UAV placement has generally overlooked the mobility aspects of the ground users in a disaster scenario. Further, in order to facilitate UAV enabled communication network, a practical fly-hover-and-communicate protocol has been proposed in [10]. In this protocol, UAVs primarily have two modes of operation: flight and hover/communicate. In the hovering or communication mode, UAVs can provide coverage to the ground users, whereas in the flight mode, there will be no coverage. Hence, with respect to the UAV placement problem, if the next optimal UAV location is far away from the current UAV location the flight time of UAVs will increase. As stated in [11], the delay in UAV to ground communication networks is primarily due to the UAV flight time, which in turn lowers the coverage time. Consequently, the flight time of UAVs is a crucial parameter in UAV placement problems. However, most of the prior works, on optimization of 3-D placement of UAVs in a disaster scenario, have considered the UAV flight time constraint. This work overcomes the above drawback by proposing a ground user mobility aware multi-UAV placement strategy for a disaster-resilient communication network which also takes into account the UAV flight time constraint.

A. Related Work and Motivation

Disaster-resilient communication networks, also referred as public safety communication (PSC) networks, are imperative to minimize the post-disaster damages. The legacy PSC networks can be broadly categorized as satellite communication networks, locally deployed resource unit (LDRU) based PSC networks and ad-hoc PSC networks [12]. Satellite communication networks require the use of specialized satellite phones that are expensive. Further, satellite communication support very low data rates [2]. LDRU based PSC networks involve the installation of fixed or movable resource units. These resource units contain a transceiver, routers, servers and a power source for establishing a communication network. However, the installation process can take up to a few days, which is not desirable. Another possible solution is the ad-hoc PSC network such as mobile ad-hoc network (MANET) and wireless mesh network (WMN) that requires no infrastructure. In ad-hoc networks, connectivity between different nodes in the network is established using multi-hop routing. This multi-hop routing is carried out in a distributed manner; hence, ad-hoc networks are energy inefficient [13]. Ad-hoc networks are also susceptible to security threats as they utilize the technologies like Wi-Fi that are not developed on the basis of PSC requirements.

As mentioned before, LTE based PSC networks are considered as a promising solution for post-disaster operations. In inaccessible and remote areas, post-disaster, UAV-BSs can play a key role [14]. Authors in [15] have developed a statistical framework to characterize and model UAV based communication networks in the wake of a disaster where they considered a clustered deployment of ground users. However, the ground user mobility can profoundly impact the network performance if the placement/location of UAVs is not optimized with the change in the ground user locations. This limitation was somewhat mitigated by the work in [16]. UAV coordinates were optimized to maximize the sum throughput using reinforcement learning where the user mobility was modelled using random walk model. In the performance analysis presented in [16], the mobility model assumes that the users are allowed to move anywhere in the simulated area. However, the above is not true for the user movements in a disaster-affected area. In disaster-affected areas, user movements are generally restricted, hence there is a need to consider a disaster-specific user mobility model for optimal UAV placement.

In this work, we propose a UAV based disaster-resilient communication network and optimize the 3-D placement of multiple UAVs in order to maximize the number of ground users covered in a disaster-affected area while taking into account the UAV flight time constraint. Unlike the prior works on UAV placement in a disaster scenario, the proposed strategy considers a disaster-specific ground user mobility model. Specifically, in this work, the emergency first responders (EFRs) are considered as the ground users and their mobility is modeled in the disaster-affected area. We demonstrate the results for single-UAV and multi-UAV scenarios in terms of average number of covered users and average coverage time in a disaster-resilient network. To the best of our knowledge, the proposed work is first of its kind for multi-UAV placement which utilizes a disater-specific user mobility model and also considers a flight time constraint for UAVs.

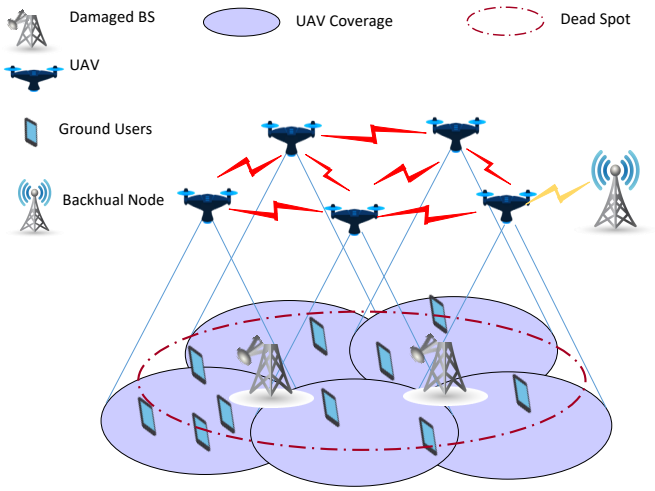

Fig. 1. Network Model.

II. Network Model

We consider a disaster scenario with damaged cellular infrastructure as shown in Fig. 1. For the ground users (in this work, EFRs) to communicate with each other as well as with the disaster control room, a disaster-resilient network is established which consists of multiple UAVs. The set $\mathcal{U}$ of UAVs act as flying BSs and are present in a 3-D space. A ground user in set U, present in the 2-D space, is said to be covered by a UAV if it is present within the coverage radius of the UAV. Hence, as the ground users move over time, UAV locations need to be updated in order to provide coverage to the ground users. As mentioned in Section I, UAVs are either in flight or hover mode. It is assumed that the ground users[1] periodically update their locations on the cloud [17]. Further, it is assumed that UAVs and users are allocated independent time-frequency resources for operation. In case of disaster, the network topology information can be utilized by the centralized software defined network (SDN) to route the traffic of UAVs [18]. The centralized SDN controller also manages the control signals to the UAVs. Further, an active BS, closest to a UAV deployed in the disaster area, can act as the backhual node [19]. UAVs can receive the control signals via inter-UAV[2] and UAV to backhual node links.

As mentioned before, the mobility of the ground users impacts the coverage performance of the network. Hence, the modelling of the ground users' mobility in a disaster scenario

[1]Specifically, EFRs can be equipped with satellite devices like satellite emergency notification device (SEND).

[2]There exists inter-UAV links as shown in Fig. 1 [20].

is required to do an efficient analysis of the UAV placement strategy.

A. Disaster Mobility Model

We adapt the mobility model for disaster area scenarios as given in [21] where the disaster area is divided into different zones based on the task to be performed in each zone. The disaster mobility model has been illustrated in Fig. 2. Zone 1 i.e., the incident site, consists of the disaster-affected people that need to be rescued. The affected people are taken to the zone 2 i.e., patient waiting area, where they are provided with the initial diagnosis and first aid treatment. Zone 3 i.e., the casualties clearing station, consists of the affected people who may need immediate care and hospitalization, and should be taken to the hospital. Zone 4 i.e., the technical operational command consists of the group of volunteers that strategize the search and rescue operations. Depending on the disaster rescue strategies, ground users will be assigned different zones. Similar to [21], we consider two types of ground users: stationary and transport ground users. Stationary ground users are restricted to a specific zone whereas transport ground users can move between two adjacent zones in a cyclic manner, i.e., zone j to zone $j+1$ and back to zone j, $j \in \{1,2,3\}$. In our work, we assume that the ground users move in random directions and with random velocities within the assigned zones. Ground users walk from one location to another, take a pause at the new location to perform a task and then move to a different location. This means the walk time and pause time occur alternately. However, for the ease of analysis, the walk time, t_{walk} of a ground user is kept constant and is assumed to be same for all ground users. Further, after each transition, the ground users are assumed to pause for a fixed amount of time. We term this as a synchronized mobility scenario, wherein the ground users walk and pause at the same time.

As mentioned above, depending on the user mobility, UAV locations need to be updated at regular intervals [16]. Due to the transitions during t_{walk} interval user locations will be more dynamic; hence, let the optimal UAV placement decision be taken at the beginning of each t_{pause} of the ground users. This will ensure that the UAV placement decisions remain optimal for a longer time. Hence, the time interval between two decisions, t_{int} consists of one t_{pause} and t_{walk} interval, i.e., $t_{int} = t_{pause} + t_{walk}$. Further, as mentioned above, UAV placements will not be optimal during t_{walk} interval. Hence, t_{pause} must consist of UAV flight time (t_{fly}) and coverage time (t_{cov}), where t_{cov} denotes the time within which maximum users are covered by UAVs. Therefore, in proposed analysis, two independent timelines denoting UAV operation and ground user mobility have been utilized. Specifically, UAVs' operation with parameters t_{fly} and t_{cov}, and ground users mobility with parameters t_{pause} and t_{walk} have been coupled together as a single timeline of UAV placement as illustrated in Fig. 3. At the n^{th} decision instant, optimal UAV locations are determined for the upcoming n^{th} pause time in the network. It may be noted that unlike t_{pause} and t_{walk}, t_{fly} and t_{cov} are random variables and there values depend on the

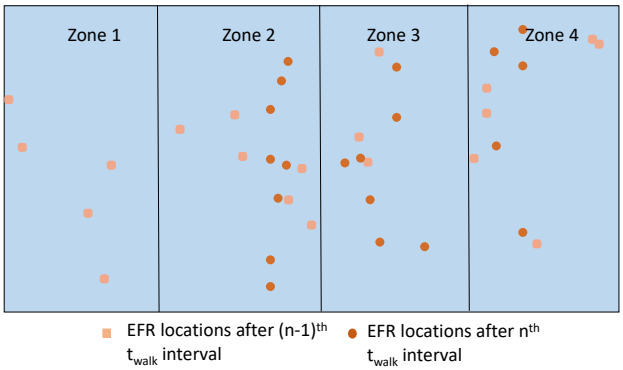

Fig. 2. Zone-wise representation of Disaster Area

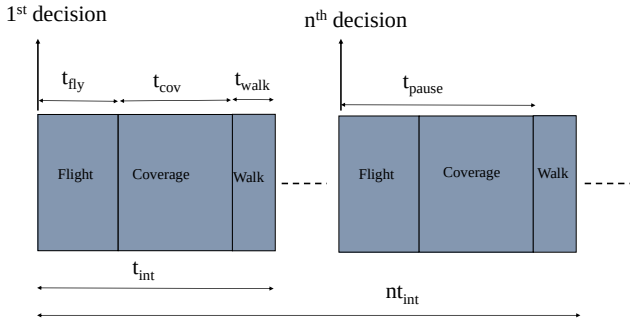

Fig. 3. Illustration of UAV Placement timeline.

optimal UAV placements. Hence, in the optimization problem, the permissible limit of t_{fly} must be set less than t_{pause} to have a non-zero t_{cov}.

III. Problem Formulation

The aim is to find the optimal placement of the UAVs to maximize the covered users such that t_{fly} constraint is met. The coordinates of the k^{th} user (represented by 'square' in Fig. 4) at the n^{th} decision instant are $(x_k^u(n), y_k^u(n))$. Let the optimal coordinates of the i^{th} UAV after the n^{th} decision

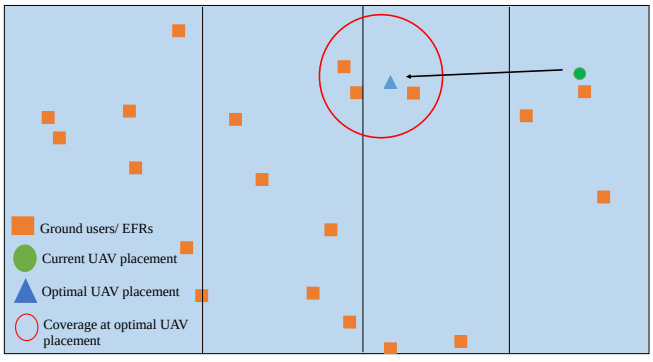

Fig. 4. 2-D illustration of the ground users along with a UAV's current and new placement.

instant be $(x_i(n), y_i(n), z_i(n))$ where $(x_i(n), y_i(n))$ denotes the horizontal placement of UAV and $z_i(n)$ denotes the UAV altitude in the 3-D space. However, for a given quality of service (QoS) requirement, as shown in [22], to maximize the coverage evaluation of the optimal altitude, $z_i(n)$ can be decoupled from the horizontal placement, $(x_i(n), y_i(n))$ of UAV in the 2-D plane. The QoS requirement is the pathloss, PL_{th} which should not be exceeded[3]. Let all the UAVs be present at the optimal altitude, z_{opt} and have a maximum coverage radius R. Hence, we will focus on the 2-D placement of UAVs in the horizontal plane where $x_i(n)$ and $y_i(n)$ are continuous variables.

In Fig. 4, 'circle' represents the current 2-D placement of a UAV, $(x_i^*(n-1), y_i^*(n-1))$ which was optimal for the $(n-1)^{th}$ t_{int} interval. The 'triangle' denotes the newly selected placement of a UAV at the n^{th} decision instant. Let I_{ik} be the distance between k^{th} user's location at the n^{th} decision instant and i^{th} UAV's location selected at the n^{th} decision instant i.e., the distance between the triangle and each of the squares in Fig. 4. Also, I_i denotes the distance between the i^{th} UAV's optimal location at the $(n-1)^{th}$ decision instant and i^{th} UAV's location selected at the n^{th} decision instant[4].

$$I_{ik} = \sqrt{\left(x_k^u(n) - x_i(n)\right)^2 + \left(y_k^u(n) - y_i(n)\right)^2} \quad (1)$$

$$I_i = \sqrt{\left(x_i(n) - x_i^*(n-1)\right)^2 + \left(y_i(n) - y_i^*(n-1)\right)^2} \quad (2)$$

The formulated optimization problem at the n^{th} decision instant is given in (3a)-(3e). (3a) is the number of users covered by the UAVs where $\mathbb{1}()$ is an indicator function that is '1' when a user is within the coverage of a UAV. (3b) is the flight time constraint that ensures that $t_{fly} = I_i/V_{uav}$ is less than or equal to t_{fly}^{max} where t_{fly}^{max} is the permissible limit on t_{fly}. The constraint (3c) is applied such that a ground user is only served by a single UAV. The UAV's x and y coordinates should be within the range $[x_{min}, x_{max}]$ and $[y_{min}, y_{max}]$ as accounted for in (3d) and (3e), respectively.

$$\underset{\{x_i(n), y_i(n)\}}{\text{maximize}} \quad \sum_i \sum_k \mathbb{1}(I_{ik} \le R),\ i \in \mathcal{U}, k \in U \quad (3a)$$

$$\text{subject to} \quad \frac{I_i}{V_{uav}} \le t_{fly}^{max},\ \forall i \in \mathcal{U}, \quad (3b)$$

$$\sum_i \mathbb{1}(I_{ik} \le R) \le 1,\ \forall k \in U, i \in \mathcal{U}, \quad (3c)$$

$$x_{min} \le x_i(n) \le x_{max},\ \forall i \in \mathcal{U}, \quad (3d)$$

$$y_{min} \le y_i(n) \le y_{max},\ \forall i \in \mathcal{U} \quad (3e)$$

The objective function (3a) and constraint (3c) can be reformulated by introducing a binary decision variable, Y_k^i to replace the indicator function as shown in (4a) and (4d), respectively. Consequently, a new constraint (4b) is introduced to take care that the condition $I_{ik} \le R$ is met. Here, M is a large constant. If $I_{ik} \le R$ then Y_k^i will have value 1. Otherwise, Y_k^i will be 0. Specifically, Y_k^i is an association variable which decides the users to be served by a UAV. The constraints (4e) and (4f) are same as constraints (3d) and (3e), respectively. Constraint (4g) is to ensure that Y_k^i has binary values. The optimization problem consists of continuous variables $x_i(n)$, $y_i(n)$ and binary/integer variables Y_k^i. Further, the objective function (4a) is linear and the constraints (4b) and (4c) are quadratic. Hence, this optimization problem is a mixed-integer quadratically constrained problem (MIQCP) [23]. The formulated problem (4a)-(4g) can be solved using IBM CPLEX solver because, in our case, the objective function is linear and the quadratic constraints are convex.

$$\underset{\{x_i(n), y_i(n), Y_k^i\}}{\text{maximize}} \quad \sum_i \sum_k Y_k^i,\ i \in \mathcal{U}, k \in U \quad (4a)$$

$$\text{subject to} \quad I_{ik} - (1 - Y_k^i)M \le R,\ \forall i \in \mathcal{U}, \forall k \in U, \quad (4b)$$

$$\frac{I_i}{V_{uav}} \le t_{fly}^{max},\ \forall i \in \mathcal{U}, \quad (4c)$$

$$\sum_i Y_k^i \le 1,\ \forall k \in U, i \in \mathcal{U}, \quad (4d)$$

$$x_{min} \le x_i(n) \le x_{max},\ \forall i \in \mathcal{U}, \quad (4e)$$

$$y_{min} \le y_i(n) \le y_{max},\ \forall i \in \mathcal{U}, \quad (4f)$$

$$Y_k^i \in \{0, 1\},\ \forall i \in \mathcal{U}, \forall k \in U \quad (4g)$$

TABLE I
USER PLACEMENT IN DISASTER-AFFECTED AREA

	Users = 10		Users = 20	
	Stationary	Transport	Stationary	Transport
Zone 1	0	2	0	8
Zone 2	2	2	4	2
Zone 3	2	0	3	0
Zone 4	2	0	3	0

IV. SIMULATION RESULTS

In this section we analyze the performance of the proposed multi-UAV placement strategy for disaster-resilient communication network. We consider a disaster area of size 900×500 sq. m in a dense urban environment. Zone 1 has dimensions 300×500 sq. m and rest of the zones have dimensions 200×500 sq. m each. Table I states the zone wise assignment of the ground users considered in our analysis. A ground user is either a stationary or transport node as explained in Section II. The other simulation parameters are provided in Table II. We assume that t_{pause} = 60 seconds, t_{walk} = 40 seconds and the user speed, v_u is uniformly distributed in [2, 3] m/s. A ground user is covered by a UAV when the pathloss does not exceed PL_{th}. Further, UAVs are assumed to fly at a constant speed, V_{uav}. We consider $V_{uav} = 18$ m/s unless otherwise

[3]For the air-to-ground (AtG) channel model and optimal altitude evaluation interested readers may refer to [22].

[4]It is assumed while travelling from one location to another UAVs follow a straight line trajectory.

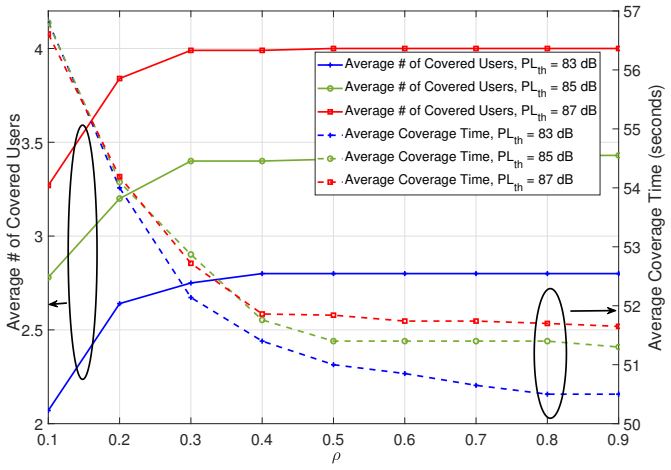

Fig. 5. Performance of proposed UAV Placement Strategy with 10 users and single UAV, t_{pause} = 60 seconds.

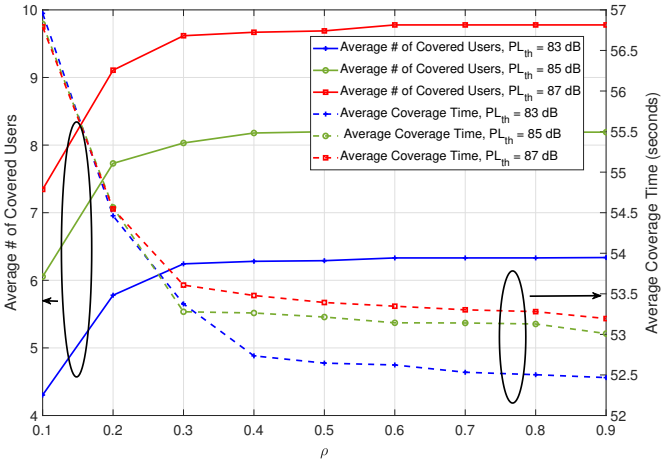

Fig. 6. Performance of proposed UAV Placement Strategy with 20 users and single UAV, t_{pause} = 60 seconds.

stated [24]. The simulation results are averaged over two hours of UAV operation in the disaster-affected area.

We know from Section II that t_{fly}^{max} must be less than t_{pause} to have a non-zero t_{cov}. Let us analyze the network for a range of t_{fly}^{max} by setting $t_{fly}^{max} = \rho t_{pause}$ where $\rho = \{0.1, 0.2, \cdots, 0.9\}$. Fig. 5 exhibits the performance of the proposed UAV placement strategy with a single UAV. It can be observed that with increase in ρ or t_{fly}^{max}, the average number of covered users increases whereas the average coverage time

TABLE II
SIMULATION PARAMETERS

Parameter	Value
t_{pause}	60 seconds
t_{walk}	40 seconds
PL_{th}	83, 85 and 87 dB (Dense urban environment)
V_{uav}	8 to 18 m/s
v_u	[2, 3] m/s

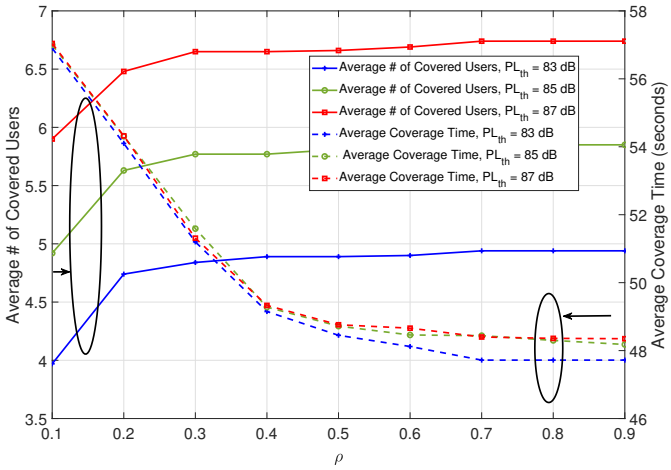

Fig. 7. Performance of proposed multi-UAV placement strategy with 10 users, t_{pause} = 60 seconds, 2 UAVs.

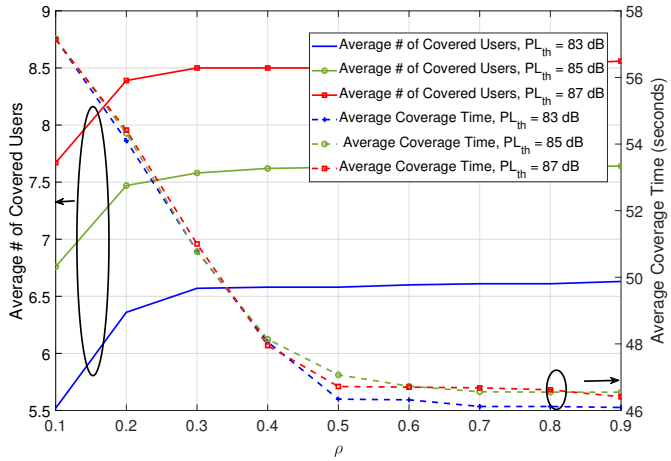

Fig. 8. Performance of proposed multi-UAV placement strategy with 20 users, t_{pause} = 60 seconds, 2 UAVs.

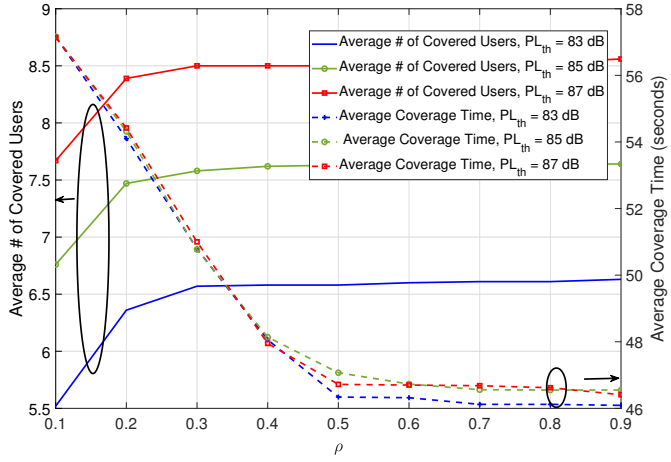

Fig. 9. Performance of proposed multi-UAV placement strategy with 10 users, t_{pause} = 60 seconds, 3 UAVs.

($\bar{t}_{cov}$) decreases. This is because an increase in ρ provides a greater flexibility for UAV movement in order to increase the number of covered users; hence, a decrease in $\bar{t}_{cov}$. There exists a trade-off between the average number of covered users and $\bar{t}_{cov}$. However, the trade-off becomes insignificant at higher ρ as the rate of increase of the average number of covered users starts to decrease at higher ρ. For instance, with 10 users, at PL_{th}= 83 dB, the rate of increase of the average number of covered users starts to decrease after $\rho = 0.3$. However, the average coverage time keeps on decreasing at a faster rate. Lower $\bar{t}_{cov}$ implies that the covered users are served by the UAVs for shorter time duration; hence, decreases the network resilience temporally. With efficient selection of the permissible limit of the UAV flight time reduction in $\bar{t}_{cov}$ is feasible.

Further, it can also be observed from Fig. 5 that $\bar{t}_{cov}$ increases with the increase in PL_{th}. This is because at higher PL_{th} the maximum coverage radius of UAV increases. Consequently, on an average, UAV does not need to displace a lot from its current location and $\bar{t}_{cov}$ is higher. It can also be observed from Fig.5 that with increase in PL_{th} the number of covered users increase. Fig. 6 exhibits the network performance with 20 users. With increase in the number of users in the network it is obvious that the average number of covered users will increase as seen in Fig. 6. Further, similar to the case with 10 users, the average number of covered users increases with ρ as well as PL_{th}.

Figs. 7, 8 and 9 present results for two UAVs with 10 users and 20 users, and three UAVs with 10 users, respectively. It can be observed that for the same ρ and PL_{th} average number of covered users increases with the number of UAVs. This is because, with increase in UAVs, the total area covered by the UAVs increases. Further, similar to the single UAV case, the rate of increase of the average number of covered users starts to decrease at higher ρ. In case of multiple UAVs, due to the (4d) constraint which requires no two UAVs to associate with the same user, UAVs need to fly a longer distance. Hence, $\bar{t}_{cov}$ is lower as compared to single UAV.

Further, we have also analyzed the proposed strategy for different values of V_{uav}. Fig. 10 demonstrates the plot for average covered user and $\bar{t}_{cov}$ at PL_{th} = 83 dB with an increase in ρ. It can be observed that at higher values of ρ, irrespective of V_{uav}, average number of covered users saturates to the same value. However, higher the UAV velocity higher is $\bar{t}_{cov}$. Given this information, it may seem advantageous to have a higher UAV velocity. However, this may not hold true. Based on the power consumption model for rotary wing UAV, a promising contender for disaster scenarios, average energy consumption per t_{pause} interval at a specific value of V_{uav} can be evaluated as follows[5] [24]:

$$E_{total}(V_{uav}) = P_h \bar{t}_{cov} + P_f(V_{uav}) \bar{t}_{fly} \tag{5}$$

[5]Energy consumption due to communication is negligible as compared to propulsion energy consumption; hence, not considered here [24]. Further, during t_{walk} UAV will always be hovering and will have a constant energy consumption irrespective of V_{uav}; hence, not considered here.

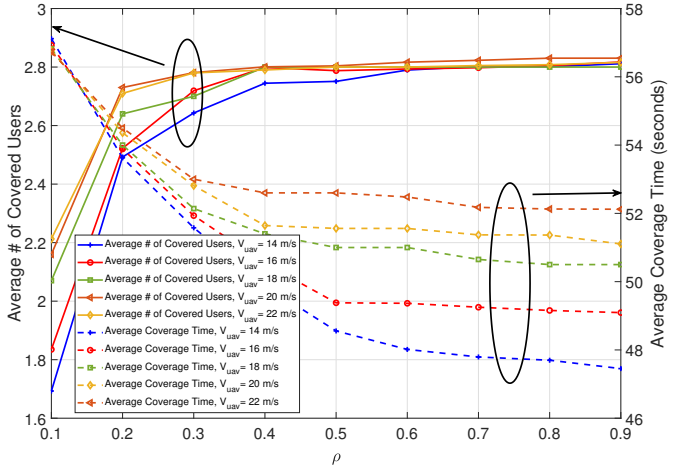

Fig. 10. Performance of proposed multi-UAV Placement Strategy with 10 users, t_{pause} = 60 seconds, single UAV and V_{uav} ranges from 14 m/s to 22 m/s.

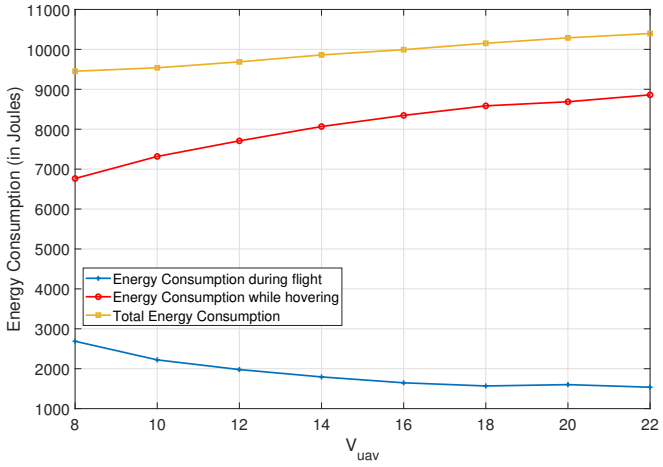

Fig. 11. Performance of proposed multi-UAV Placement Strategy with 10 users, t_{pause} = 60 seconds, single UAV and V_{uav} ranges from 14 m/s to 22 m/s.

where P_h is the power consumption due to hovering and $P_f(V_{uav})$ is the power consumption due to flight of UAV. The energy consumption is plotted in Fig. 11. On increasing V_{uav}, there is a reduction in $\bar{t}_{fly}$ and an increase in $P_f(V_{uav})$. However, the impact of $\bar{t}_{fly}$ is dominant. Consequently, the energy consumption due to flight decreases with V_{uav}. Further, on increasing V_{uav}, $\bar{t}_{cov}$ i.e., the hovering time during t_{pause} will increase and will result in increase in energy consumption due to hovering. Therefore, the overall energy consumption at the UAV increases.

V. Conclusion

We have proposed a ground user mobility aware multi-UAV placement strategy for a disaster-resilient communication network. The disaster-affected area has been divided into four zones and EFRs/ground users are assigned different zones. For developing a ground user mobility aware strategy, we have modeled the mobility of ground users within their assigned

zones. Based on the above, an optimization problem has been formulated to maximize the number of covered users while taking into account the UAV flight time constraint. We observed that there exists a trade-off between the average number of covered users and average coverage time. Further, UAV flight time constraint is more crucial in multi-UAV scenario as compared to single UAV scenario. This is due to the fact that multi-UAV scenario tend to have a lower average coverage time as compared to single UAV scenario with increase in UAV flight time permissible limit. It has also been observed that with increase in UAV velocity, for a given average number of covered users, average coverage time increases. However, the overall energy consumption at a UAV increases with increase in UAV velocity because the increase in energy consumption due to hovering surpasses the decrease in energy consumption due to flight.

REFERENCES

[1] K. Gomez, L. Goratti, T. Rasheed, and L. Reynaud, "Enabling disaster-resilient 4g mobile communication networks," *IEEE Communications Magazine*, vol. 52, no. 12, pp. 66–73, December 2014.

[2] G. Baldini, S. Karanasios, D. Allen, and F. Vergari, "Survey of wireless communication technologies for public safety," *IEEE Communications Surveys Tutorials*, vol. 16, no. 2, pp. 619–641, Second 2014.

[3] K. Flynn, "The mobile broadband standard." [Online]. Available: https://www.3gpp.org/news-events/1875-mc_services

[4] Z. Kaleem, M. Yousaf, A. Qamar, A. Ahmad, T. Q. Duong, W. Choi, and A. Jamalipour, "Uav-empowered disaster-resilient edge architecture for delay-sensitive communication," *IEEE Network*, pp. 1–9, 2019.

[5] M. Mozaffari, W. Saad, M. Bennis, Y.-H. Nam, and M. Debbah, "A tutorial on uavs for wireless networks: Applications, challenges, and open problems," 2018.

[6] R. I. Bor-Yaliniz, A. El-Keyi, and H. Yanikomeroglu, "Efficient 3-d placement of an aerial base station in next generation cellular networks," in *2016 IEEE International Conference on Communications (ICC)*, May 2016, pp. 1–5.

[7] M. Mozaffari, W. Saad, M. Bennis, and M. Debbah, "Efficient deployment of multiple unmanned aerial vehicles for optimal wireless coverage," *IEEE Communications Letters*, vol. 20, no. 8, pp. 1647–1650, Aug 2016.

[8] E. Kalantari, I. Bor-Yaliniz, A. Yongacoglu, and H. Yanikomeroglu, "User association and bandwidth allocation for terrestrial and aerial base stations with backhaul considerations," in *2017 IEEE 28th Annual International Symposium on Personal, Indoor, and Mobile Radio Communications (PIMRC)*, Oct 2017, pp. 1–6.

[9] J. Lu, S. Wan, X. Chen, and P. Fan, "Energy-efficient 3d uav-bs placement versus mobile users' density and circuit power," in *2017 IEEE Globecom Workshops (GC Wkshps)*, Dec 2017, pp. 1–6.

[10] H. He, S. Zhang, Y. Zeng, and R. Zhang, "Joint altitude and beamwidth optimization for uav-enabled multiuser communications," *IEEE Communications Letters*, vol. 22, no. 2, pp. 344–347, Feb 2018.

[11] Q. Wu, L. Liu, and R. Zhang, "Fundamental trade-offs in communication and trajectory design for uav-enabled wireless network," *IEEE Wireless Communications*, vol. 26, no. 1, pp. 36–44, February 2019.

[12] K. G. Panda, S. Das, D. Sen, and W. Arif, "Design and deployment of uav-aided post-disaster emergency network," *IEEE Access*, vol. 7, pp. 102 985–102 999, 2019.

[13] M. Tanha, D. Sajjadi, F. Tong, and J. Pan, "Disaster management and response for modern cellular networks using flow-based multi-hop device-to-device communications," in *2016 IEEE 84th Vehicular Technology Conference (VTC-Fall)*, Sep. 2016, pp. 1–7.

[14] N. Zhao, W. Lu, M. Sheng, Y. Chen, J. Tang, F. R. Yu, and K. Wong, "Uav-assisted emergency networks in disasters," *IEEE Wireless Communications*, vol. 26, no. 1, pp. 45–51, February 2019.

[15] A. M. Hayajneh, S. A. R. Zaidi, D. C. McLernon, M. Di Renzo, and M. Ghogho, "Performance analysis of uav enabled disaster recovery networks: A stochastic geometric framework based on cluster processes," *IEEE Access*, vol. 6, pp. 26 215–26 230, 2018.

[16] R. Ghanavi, E. Kalantari, M. Sabbaghian, H. Yanikomeroglu, and A. Yongacoglu, "Efficient 3d aerial base station placement considering users mobility by reinforcement learning," in *2018 IEEE Wireless Communications and Networking Conference (WCNC)*, April 2018, pp. 1–6.

[17] C. P. Hoffman, W. Cox, and T. J. Pack, "Dual-satellite emergency locator beacon and method for registering, programming and updating emergency locator beacon over the air," US Patent, US9 031 497B1.

[18] I. Bor-Yaliniz and H. Yanikomeroglu, "The new frontier in ran heterogeneity: Multi-tier drone-cells," 2016.

[19] C. T. Cicek, H. Gultekin, B. Tavli, and H. Yanikomeroglu, "Uav base station location optimization for next generation wireless networks: Overview and future research directions," 2018.

[20] B. Li, Z. Fei, and Y. Zhang, "Uav communications for 5g and beyond: Recent advances and future trends," *IEEE Internet of Things Journal*, vol. 6, no. 2, pp. 2241–2263, April 2019.

[21] N. Aschenbruck, E. Gerhards-Padilla, M. Gerharz, M. Frank, and P. Martini, "Modelling mobility in disaster area scenarios," in *Proceedings of the 10th ACM Symposium on Modeling, Analysis, and Simulation of Wireless and Mobile Systems*, ser. MSWiM '07. New York, NY, USA: ACM, 2007, pp. 4–12. [Online]. Available: http://doi.acm.org/10.1145/1298126.1298131

[22] M. Alzenad, A. El-Keyi, F. Lagum, and H. Yanikomeroglu, "3-d placement of an unmanned aerial vehicle base station (uav-bs) for energy-efficient maximal coverage," *IEEE Wireless Communications Letters*, vol. 6, no. 4, pp. 434–437, Aug 2017.

[23] S. Burer and A. Saxena, "The MILP road to MIQCP," in *Mixed Integer Nonlinear Programming*, J. Lee and S. Leyffer, Eds. New York, NY: Springer New York, 2012, pp. 373–405.

[24] Y. Zeng, J. Xu, and R. Zhang, "Energy minimization for wireless communication with rotary-wing uav," *IEEE Transactions on Wireless Communications*, vol. 18, no. 4, pp. 2329–2345, April 2019.